A STUDY ON PROGRESSIVE FAILURE ANALYSIS OF HIGH-RISE STEEL BUILDINGS USING IMPROVED APPLIED ELEMENT METHOD

Said A.Elkholy, Student Member, The University of Tokyo
Kimiro Meguro, Regular Member, The University of Tokyo

1. INTRODUCTION

The collapse of the World Trade Centre, on September, 2001, was caused by a series of very complex events, involving tremendous impact to the structure, fire explosion and resulting heat. Responding like these attacks around the world, numerous researchers are seeking new methods for simulating the collapse of those towers to understand and prevent progressive collapse of such high-rise buildings. It is very difficult or practically impossible to follow the complete collapse behaviour using numerical methods based on continuum material like FEM and BEM. Few of numerical methods can deal with collapse analysis, like EDEM[1] and AEM[2),3)], which can simulate collapse behaviour of reinforced concrete structures; however the application of AEM for steel structure is still limited. For that reason, the authors attempted to improve the exciting code of AEM to be able to follow the behaviour of steel structure up to the complete collapse by modifying element type. The new element reduces the number of elements, thus further reducing the CPU time required. The accuracy of the new element is tested and validated under both static and dynamic loading situations. The proposed numerical method also takes into account contact-impact, recontact and inertia effects. Collapse analysis for high-rise steel structure has been introduced in this paper.

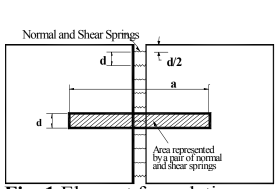

Fig. 1 Element formulation

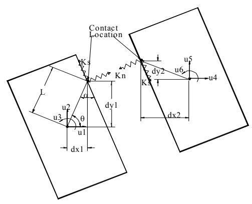

Fig. 2 Spring connectivity

$$\begin{bmatrix} \mathrm{Sin}^2(\theta+\alpha)K_n + \mathrm{Cos}^2(\theta+\alpha)K_s & -K_n\mathrm{Sin}(\theta+\alpha)\mathrm{Cos}(\theta+\alpha) + K_s\mathrm{Sin}(\theta+\alpha)\mathrm{Cos}(\theta+\alpha) & \mathrm{Cos}(\theta+\alpha)K_s L\mathrm{Sin}(\alpha) - \mathrm{Sin}(\theta+\alpha)K_n L\mathrm{Cos}(\alpha) \\ -K_n\mathrm{Sin}(\theta+\alpha)\mathrm{Cos}(\theta+\alpha) + K_s\mathrm{Sin}(\theta+\alpha)\mathrm{Cos}(\theta+\alpha) & \mathrm{Sin}^2(\theta+\alpha)K_s + \mathrm{Cos}^2(\theta+\alpha)K_n & \mathrm{Cos}(\theta+\alpha)K_n L\mathrm{Cos}(\alpha) + \mathrm{Sin}(\theta+\alpha)K_s L\mathrm{Sin}(\alpha) \\ \mathrm{Cos}(\theta+\alpha)K_s L\mathrm{Sin}(\alpha) - \mathrm{Sin}(\theta+\alpha)K_n L\mathrm{Cos}(\alpha) & \mathrm{Cos}(\theta+\alpha)K_n L\mathrm{Cos}(\alpha) + \mathrm{Sin}(\theta+\alpha)K_s L\mathrm{Sin}(\alpha) & L^2\mathrm{Cos}^2(\alpha)K_n + L^2\mathrm{Sin}^2(\alpha)K_s \end{bmatrix} \quad \textbf{(3)}$$

2. APPLIED ELEMENT METHOD (AEM)

In AEM, structure is modelled as an assembly of small elements that are made by dividing of the structure virtually. Adjacent elements are assumed to be connected by pairs of normal and shear springs located at contact locations that are distributed around the element edges. Each pair of springs totally represents stresses and deformations of a certain area (hatched area in **Fig. 1**) of the studied elements. Therefore, the normal and shear stiffness can be determined by **Eq. (1)**:

$$K_n = \frac{E*d*T}{a} \text{ and } K_s = \frac{G*d*T}{a} \qquad (1)$$

where d = distance between each springs; a = length of representative area; E and G = Young's and shear modulus of the material, respectively; and T is the thickness of element.

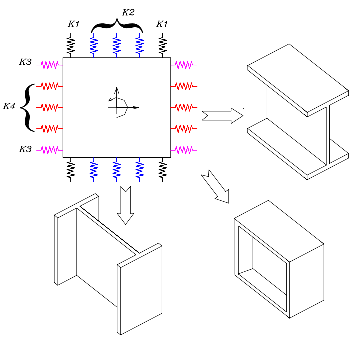

Fig. 3 Element Shape for Improved AEM

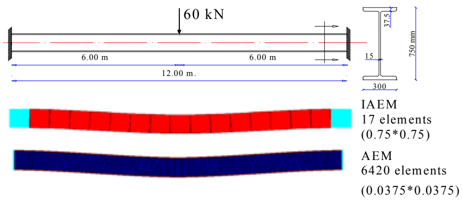

Fig. 4 Fixed beam Example

Table 1. Comparison between AEM and IAEM

	Number of elements	Element size (cm^2)	CPU Time Required	Defalcation (mm.)	Error Ratio (%)
AEM	6420	3.75*3.75	154 sec	1.138	+9.30%
IAEM	17	75*75	Less than 1 secc.	0.987	-5.20 %

3. IMPROVED APPLIED ELEMENT METHOD (AEM)

In this method more flexibility was added to AEM to be able to use different characteristic for each spring to match any change in the thickness in any part of structure cross sections. That kind of modification allows using element with large size, having the same cross sectional parameter like normal, shear and bending stiffness. For that reason, the normal and shear stiffness for each spring can be determined by **Eq. (2)**, which is more generalized than **Eq. (1)**.

$$K_n^i = \frac{E*d*T_n^i}{a} \text{ and } K_s^i = \frac{G*d*T_s^i}{a} \qquad (2)$$

where: T_n^i and T_s^i are the thickness represented by the spring *i* for normal and shear cases, respectively. That difference in the value of T_n^i and T_s^i owes to the change in effective area for both of normal and shear directions. As shown in **Fig. 2**, each element has three DOFs, which represent the rigid body motion of the element; each pair of normal and shear springs affects six DOFs depending on the stiffness of each spring and the location of spring stiffness. **Eq. (3)** shows the components of the upper left quarter of the (6x6) stiffness matrix of any pair of contact springs. However, the global stiffness matrix is determined by summing up the stiffness matrices of individual pair of springs around all elements.

Although in this method, we can change the characteristics of all springs surrounding any element, in practical use, the changing in the corner springs only is enough for simulating the steel flanged sections. From **Fig.3**, we can see that changing in the ratios of (K1/K2) and (K3/K4) can control on the stiffness of any element. That kind of improvement allows using many different flanged steel sections**.** Moreover, the element size may be chosen as the height of each cross section. That means elements with large size can be used in order to decrease the required number of elements and CPU time. To verify the

Key words: Applied Element Method, AEM, Collapse analysis, Progressive Failure
Institute of Industrial Science, The University of Tokyo, 4-6-1 Komaba, Meguro-Ku, Tokyo 153-8505, Japan Tel: 03-5452-6437, Fax: 03-5452-6438)

proposed model, analysis is carried out in linear static and dynamic load conditions. The results are compared with theoretical ones.

4. VREVICATION FOR STATIC CASE

A 2-D steel beam, as shown in **Fig. 4,** is studied to check the accuracy of Improved AEM (IAEM). The dimensions, supports, loading conditions, and cross section are shown in the figure. The defection at the mid span of the beam was calculated by using both previous AEM and IAEM versions. The Young's Modulus is assumed as 2.00×10^5 MPa and elastic analysis was performed. Element size is taken as total height of the cross section in IAEM case. The ratio between outer and inner springs' stiffness was taken as 20 (the same ratio between flange width and web thickness). However, in previous version of AEM, which use constant thickness per element, size of element is taken as flange thickness. The results are compared with the theoretical results. A brief comparison between AEM and IAEM is listed in **Table 1**. The percentage of error in the maximum displacement is also shown in the table. From the table, we can see that even by using much less number of elements, the accuracy was better with the IAEM compared with AEM.

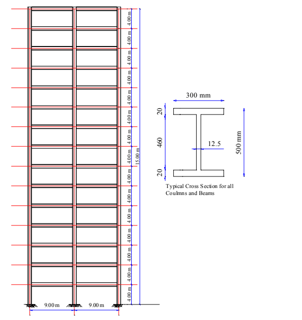

Fig.(5) 15-Story Two Bay Frame

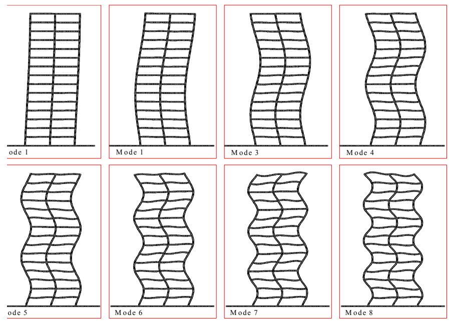

Fig. (6) First Eight modes calculated using IAEM

5. IAEM FOR DYNAMIC CASE

In IAEM, the mass matrix and the polar moment of inertia of each element have been idealized as lumped at the element centroid. The values of those lumped mass in each DOF direction can be calculated by summing the effect of small segmental mass represented by each spring considering the change of springs' thickness. **Equation 4** represents the value of lumped mass in each DOF.

$$\begin{bmatrix} M1 \\ M2 \\ M3 \end{bmatrix} = \begin{bmatrix} D^2 * t_{av} * \rho \\ D^2 * t_{av} * \rho \\ \dfrac{D^4 \cdot \rho}{nsp} \cdot \sum_{i=1}^{i=nsp} \left(\dfrac{t_i^x}{12} + \dfrac{t_i^y}{12} \right) \end{bmatrix} \qquad (4)$$

where: M_1 and M_2 are the element mass; M_3 is the element polar moment of inertia around the centroid; D is the element size; and t_{av} and ρ are the average thickness and the material density of the element, respectively.

In order to evaluate the accuracy of IAEM in dynamic analysis, a 15 story- two bay two-dimensional frame structure (presented in **Fig. 5**) is considered in this study. Young's modulus of 2×10^5 MPa is used. The analysis is performed using 870 elements; however 543,750 elements should be used to simulate the same structure by using previous version of AEM. The modal analysis is performed directly on the linear constant stiffness. The fundamental frequencies of the structure are calculated and listed in **Table 2.** Those values are computed very well with those calculated by using FEM. The first 8^{th} mode shapes are shown in **Fig. 6**.

Table 2: The Results of Model Analysis (Frequency, Hz)

Mode	1	2	3	4	5	6	7	8
FEM	2.817	8.627	15.129	21.903	29.316	37.229	46.253	55.320
IAEM	2.851	8.761	15.376	22.255	29.765	37.229	46.773	56.042
Diff. %	1.21	1.55	1.63	1.61	1.53	0.00	1.12	1.31

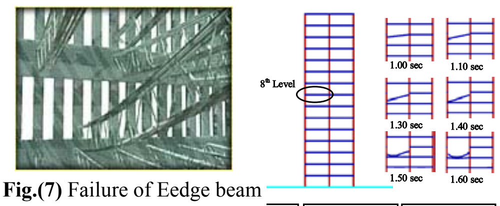

Fig.(7) Failure of Eedge beam

6. PROGRESSIVE FAILURE ANALYSIS

The steel frame building is analysed by **IAEM** in this study. The main purpose of the analysis is to check the reliability of the proposed method and to check if the progressive failure will occur due to partial damage beyond one story level. The progressive failure has been occurred due to local failure, as shown in **Fig. 7**, which assumed to be in the eighth floor level. This kind of initial damage in that location may be produced due to sever fire near to that location. Complete failure of the whole structure can be followed by IAEM as shown in **Fig. 8**.

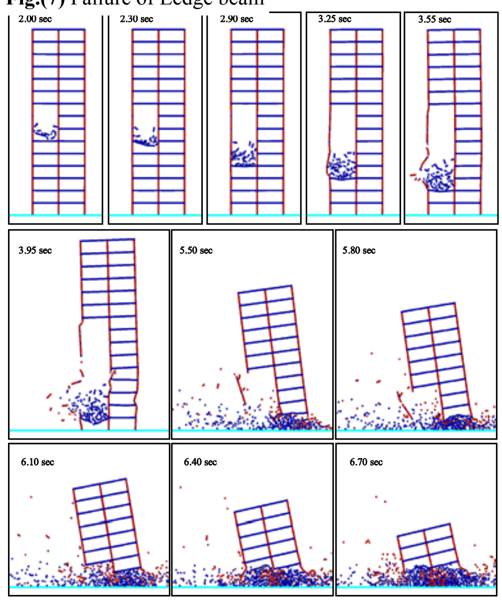

Fig.(8) Failure Process of 15 Story Frame under Local Damage in 8^{th} floor level

7. CONCLUSIONS

This paper presented and discussed new extension to AEM (IAEM). The verification examples indicate that IAEM has better accuracy, less computational effort, and a wider applicability for structural analysis, especially for studying high rise steel buildings than conventional methods.

References

1)Meguro K. and Hakuno M.(1989). "Fracture analyses of structures by the modified distinct element method." *Structural Eng./Earthquake Eng.*, Vol. 6. No. 2, 283-294.

2)Meguro K. and Tagel-Din H. (2001)."Applied Element Simulation of RC Structures under Cyclic Loading." *Journal of Structural Engineering, ASCE,* Vol. 127, No. 11, 1295-1305.

3)Meguro K. and Tagel-Din H. (2002). "Applied Element Method used for large displacement structural analysis." *Journal of Nature Diaster Science,* Vol. 24, No. 1, 25-34.